Activation of olfactory-type cyclic nucleotide-gated channels is highly cooperative

Vasilica Nache[1], Eckhard Schulz[2], Thomas Zimmer[1], Jana Kusch[1], Christoph Biskup[1], Rolf Koopmann[1], Volker Hagen[3] and Klaus Benndorf[1]

[1] *Institut für Physiologie II, Friedrich-Schiller-Universität Jena, D-07743 Jena, Germany*
[2] *Fachhochschule Schmalkalden, Fachbereich Elektrotechnik, Blechhammer, D-98754 Schmalkalden, Germany*
[3] *Forschungsinstitut für Molekulare Pharmakologie, Robert-Rössle-Str. 10, D-13125 Berlin, Germany*

Cyclic nucleotide-gated (CNG) ion channels play a key role in the sensory transduction of vision and olfaction. The channels are opened by the binding of cyclic nucleotides. Native olfactory CNG channels are heterotetramers of CNGA2, CNGA4, and CNGB1b subunits. Upon heterologous expression, only CNGA2 subunits can form functional homotetrameric channels. It is presently not known how the binding of the ligands to the four subunits is translated to channel opening. We studied activation of olfactory CNG channels by photolysis-induced jumps of cGMP or cAMP, two cyclic nucleotides with markedly different apparent affinity. It is shown that at equal degree of activation, the activation time course of homotetrameric channels is similar with cGMP and cAMP and it is also similar in homo- and heterotetrameric channels with the same cyclic nucleotide. Kinetic models were globally fitted to activation time courses of homotetrameric channels. While all models containing equivalent binding sites failed, a model containing three binding sites with a ligand affinity high–low–high described the data adequately. Only the second binding step switches from a very low to a very high open probability. We propose a unique gating mechanism for homotetrameric and heterotetrameric channels that involves only three highly cooperative binding steps.

(Received 9 June 2005; accepted after revision 29 July 2005; first published online 4 August 2005)
Corresponding author K. Benndorf: Institut für Physiologie II, Friedrich-Schiller-Universität Jena, Kollegiengasse 9, D-07743 Jena, Germany. Email: klaus.benndorf@mti.uni-jena.de

Cyclic nucleotide-gated (CNG) ion channels mediate phototransduction in photoreceptors and chemotransduction in olfactory neurones (Zagotta & Siegelbaum, 1996; Kaupp & Seifert, 2002). The minimum gating model of CNG channels comprises the binding of an unknown number of ligands which promotes a conformational change associated with channel opening (Li *et al.* 1997). These processes can be described by kinetic models. Models of the sequential type assume that the channel opens only when all binding sites are occupied by the ligands. However, CNG channels were shown to open also in the absence of any activating ligand (Picones & Korenbrot, 1995; Tibbs *et al.* 1997). Although the open probability for these spontaneous openings is only very low, it favours cyclic allosteric models, such as the Monod-Wyman-Changeux (MWC) model (Monod *et al.* 1965). When applied to CNG channels, allosteric models assume that the binding sites of the four subunits are equivalent but that the ligand affinity is higher in the open than in the closed states by an allosteric factor f (Li *et al.* 1997). However, the open probabilities for partially liganded channels were not in the ratios predicted by the MWC model (Ruiz & Karpen, 1997; Liu *et al.* 1998). Instead, the coupled-dimer (CD) model has been proposed in which the two binding sites of a dimer are equivalent and the channel opens only when both dimers are activated (Liu *et al.* 1998). Alternatively, based on single-channel data, the gating of CNGA2 channels has been explained by cooperative ligand binding: One or two ligands bind to the closed channel and a further ligand binds to the open channel (Li & Lester, 1999). All these measurements were performed under steady-state conditions.

Further insight into the activation gating of CNGA2 channels can be expected by studying currents under non-equilibrium conditions, i.e. by changing the cyclic nucleotide concentration in a step-like fashion and studying the activation kinetics of the macroscopic current. Karpen *et al.* (1988) applied this technique to native rod photoreceptor channels and they interpreted their results with a sequential model containing three cooperative binding steps followed by an allosteric transition.

 DOI: 10.1113/jphysiol.2005.092304

We benefited from the superior properties of coumarinylmethyl esters of cGMP and cAMP which allowed us to perform jumps of the free ligand concentration from zero to constant values, covering the whole relevant range of the concentration–response relationships of the channels. We show for homotetrameric CNGA2 channels that the binding of only three ligands is required to describe the activation time courses, that the ligand binding is highly cooperative, and that the allosteric reaction is similarly fast for cGMP and cAMP. Moreover, heterotetrameric CNGA2/A4/B1b channels are activated with the same kinetics as homotetrameric CNGA2 channels.

Methods

Oocyte preparation and cRNA injection

Oocytes were obtained surgically under anaesthesia (0.3% 3-aminobenzoic acid ethyl ester) from adult females of *Xenopus leavis*. The condition of the animals was monitored between the ovarian lobe resections and care was taken to avoid distress or infection. The animals were humanely killed by decapitation under anaesthesia, following final collection of oocytes. The procedures had approval from the authorized animal ethical committee of the Friedrich Schiller University Jena. The oocytes were treated for 60–90 min with 1.2 mg ml^{-1} collagenase (Type I, Sigma, St Louis, MO, USA) and manually dissected. They were injected with 40–70 nl of a solution containing cRNA specific for the respective channel. We used cRNA specific for bovine CNGA2 channels or a mixture of cRNAs specific for native rat olfactory channels with CNGA2: CNGA4: CNGB1b of 2 : 1 : 1. The respective accession numbers are X 55010, AF 126808, U 12623, and AF 068572. The oocytes were incubated at 18°C in Barth medium until experimental use within 6 days after injection.

Chemicals

All chemicals were of analytical grade. cGMP and cAMP were obtained from Sigma. As caged cGMP and caged cAMP we used the [7-(diethylamino)coumarin-4-yl]methyl esters of cGMP (DEACMcGMP) and cAMP (DEACMcAMP). The wavelengths of the light used for photolysis were 320–480 nm. Synthesis and the superior physicochemical properties of these compounds for photolysis have been described elsewhere (Hagen *et al.* 2001).

Recording technique

Currents were recorded in inside-out patches with a patch-clamp technique. The patch pipettes were pulled from quartz tubing (outer diameter 1.2 mm, inner diameter 0.8 mm (macroscopic currents) or 0.4 mm (single-channel experiments)) using a laser puller (P-2000, Sutter Instrument Co., Novato, CA, USA). The pipette resistance was 0.8–2.5 MΩ or 5–25 MΩ, respectively. Recording was performed with an Axopatch 200B amplifier (Axon Instruments, Union City, CA, USA). All experiments were performed with the same recording solution in the bath with the pipette containing (mM): 150 KCl, 1 EGTA, 5 Hepes, pH 7.4 with KOH. To test for possible background channel activity, each excised patch was first exposed to a solution containing no cyclic nucleotide. Then the maximum current was activated with free cyclic nucleotide (100 μM cGMP or 1000 μM cAMP for CNGA2 channels, 700 μM cAMP CNGA1/A4/B1b channels). The currents were measured at a voltage of +100 mV.

The experimental chamber was mounted on the stage of an inverted microscope (Axiovert 100, Carl Zeiss, Jena, Germany). It was composed of two compartments (Fig. 1*A*). In the main compartment (width 8 mm) the oocyte was positioned, the sealing was performed, and all free cyclic nucleotide concentrations were administered in a laminar flow (flow rate 0.12 ml min^{-1}). The solution containing the caged cGMP was led to the main compartment in an angle of 90 deg, thereby passing the photolysis compartment (width 0.5 mm, height 1.0 mm) just before entering the main compartment. One wall of the photolysis compartment was formed by the end of a light guide (diameter 1.0 mm) and the opposite wall by a mirror. At the top side, the photolysis compartment was confined by a glass plate for light transmission when positioning the pipette under optical control. The bottom of the experimental chamber consisted of two parallel glass plates. Between these plates, thermostated water flew to control the temperature in both the main and the photolysis compartment. The temperature in both compartments was 20.3 ± 0.1°C. The experiments were viewed through the double-walled chamber bottom and the thermostated water.

Flash photolysis

Light flashes were generated by the flash-lamp system JML-C2 (Rapp OptoElectronic, Hamburg, Germany) and directed to the experimental chamber by a light guide (diameter 1.0 mm) fabricated of quartz. The time course of the light pulses shows (Fig. 1*B*) that photolysis was completed within 150 μs. This time interval of photolysis was 40 times shorter than the fastest time constant of the current signals studied herein. According to the manual for the flash-lamp system, the energy of a light pulse was 0.45–1.47 mJ.

Given by the geometry of the photolysis chamber, photolysis was performed in a cylindrical volume of 390 nl. The pipette tip was positioned in the middle of the

photolysis chamber. The solution flow through the photolysis chamber was adjusted such that the concentration of the liberated cyclic nucleotide was constant for at least 1.5 s, as evaluated by the constant amplitude of the late current. Figure 1*C* shows a respective experiment with DEACMcGMP. The next flash was elicited only after the current induced by the cyclic nucleotide had decreased to the current level in the absence of the cyclic nucleotide determined in the main chamber before the photolysis experiments. The interval between the flashes ranged from 10 to 25 s.

To determine the concentration of the free cyclic nucleotide produced by flash photolysis, for each patch the ratio of the steady-state current following a flash to the steady-state current at a saturating concentration of the free cyclic nucleotide (I_∞/I_{max}, Fig. 2*A*) was experimentally determined and inserted in the equation:

$$[\text{cyclic nucleotide}] = EC_{50}[(I_{max}/I_\infty) - 1]^{(-1/H)} \quad (1)$$

where EC_{50} and H are the half-maximum concentration and the Hill coefficient determined from the concentration–response relationship of the respective free cyclic nucleotide and channel. The current amplitude at saturating concentrations of the cyclic nucleotide was determined immediately after a light flash.

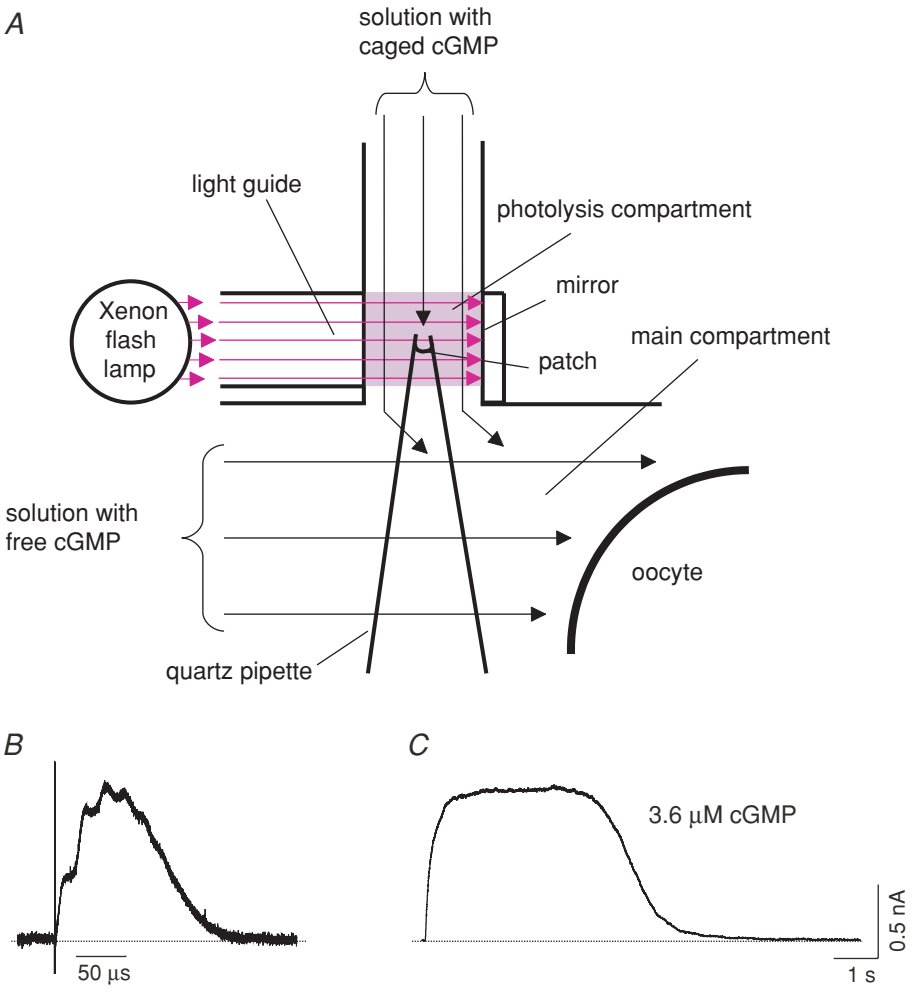

Figure 1. Method of flash photolysis of caged cyclic nucleotides
A, scheme of the experimental chamber. The chamber consists of two compartments. In the large main compartment the patch was formed and the solutions with the free cyclic nucleotide were administered. The solution with the caged cyclic nucleotide entered the small photolysis compartment from the side before flowing into the main compartment. For further explanation see text. *B*, time course of a light flash delivered by the xenon flash lamp. The trace was recorded with a photodiode. *C*, time course of a CNGA2 current activated by flash photolysis of 3.6 μM cGMP. After 4 s the concentration of the liberated cGMP decreased due to the replacement by fresh solution with the caged compound. All analyses of the activation kinetics were performed before the decrease of current started. A subsequent flash was elicited only after the current had decayed to zero.

Figure 2*B–D* shows the respective concentration–response relationships.

To rule out direct effects of the light flashes with the intensity used herein on the channels (Middendorf *et al.* 2000; Middendorf & Aldrich, 2000), CNGA2 channels were activated by free cGMP (10 μM) and the patches were exposed to 10 flashes as used for uncaging. The current amplitude was unaffected. We also examined whether the caged compounds affect the channels without uncaging. The channels were activated by free cyclic nucleotide concentrations of 2–3 times the EC_{50} value. At high concentrations the caged compounds slightly reduced the amplitude of the macroscopic current. This effect was reversible. For determination of the open probability, the measured current amplitudes were therefore corrected by amplitude factors ranging from 1.002 to 1.21.

Data acquisition and analysis

Measurements were controlled and data were collected with the ISO3 soft- and hardware (16-bit resolution; MFK Niedernhausen, Germany) running on a Pentium PC. For macroscopic currents the sampling rate was generally 2 kHz (filter 1 kHz). Single-channel activity of CNGA2 channels was recorded with a sampling rate of 20 kHz (filter 5 kHz). All currents were corrected for capacitive and very small leak components by subtracting corresponding averaged currents in the absence of a cyclic nucleotide.

The amplitude of the single-channel currents was determined by forming all-point amplitude histograms and fitting the distribution with sums of Gaussian functions. Single-channel open times were determined by setting a threshold to the 50% level of the current

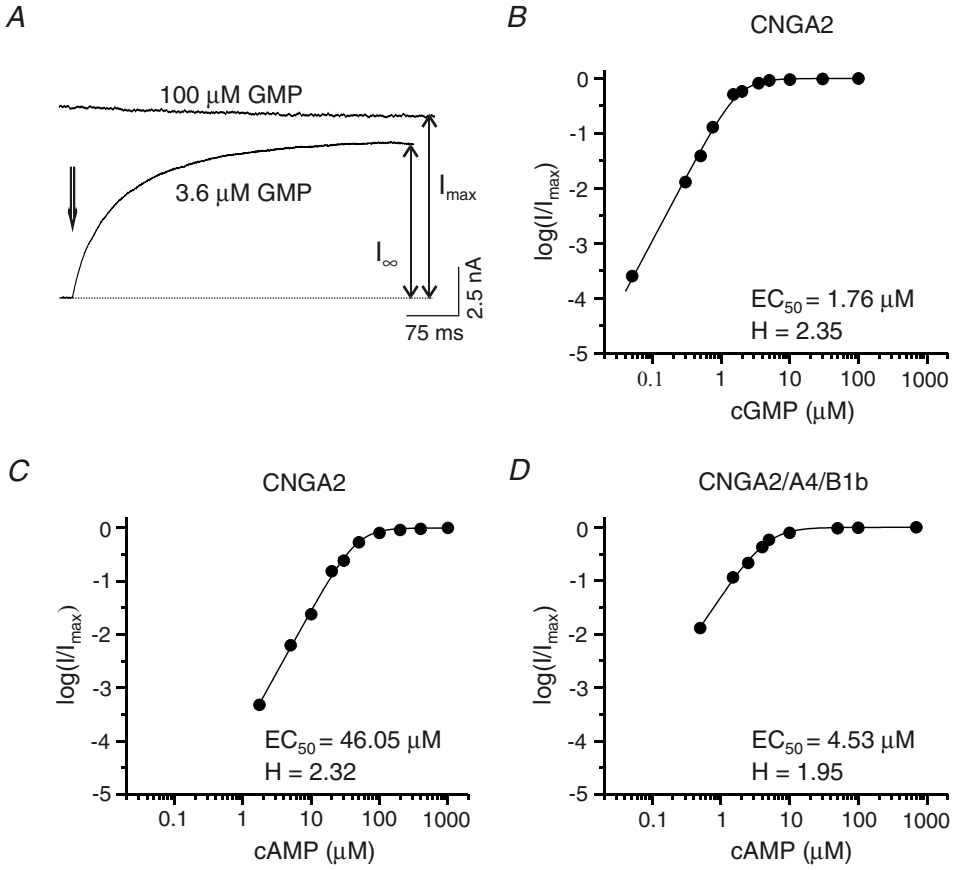

Figure 2. Determination of the free cyclic nucleotide concentration generated by flash photolysis
A, example of a CNGA2-current recording activated by cGMP in a multichannel patch. The maximum current, I_{max}, was recorded with 100 μM free cGMP. In the same patch the current was activated by a jump of cGMP from zero to 3.6 μM induced by flash photolysis of DEACMcGMP (arrow). After 400 ms the current reached the steady-state level I_∞. The ratio (I_∞/I_{max}) was inserted in eqn (1). *B*, concentration–response relationship for CNGA2 currents and free cGMP. The steady-state current (I) was recorded at the indicated concentrations and referred to the steady-state current (I_{max}) at 100 μM cGMP, which is a saturating cGMP concentration. The data points were fitted by $I/I_{max} = 1/\{(1 + (EC_{50}/[cGMP])^H\}$. EC_{50} and H are the cGMP concentration of half-maximum channel activation and the Hill coefficient, respectively. Both parameters were inserted in eqn (1). *C* and *D*, concentration–response relationships for CNGA2 and CNGA2/A4/B1b channels activated with free cAMP. EC_{50} and H were determined as described in (*B*). Each data point was obtained from 5–15 patches.

amplitude. Open-time histograms were formed and described by exponentials. The open probabilities were determined from amplitude histograms of single-channel recordings. At saturating cGMP or cAMP, the patches contained one and only one channel. In the absence of cyclic nucleotides, multichannel patches were used in which the channel number was such that amplitude histograms resolved single-channel events. Curves were fitted to the data with non-linear approximation algorithms using either the ISO3 or the Origin 6.1 (OriginLab Corp., Northampton, MA, USA) software.

Markov models were approximated to macroscopic currents that were induced by jumps of cGMP. To increase constraints, seven currents covering a wide range of open probabilities were fitted globally. The respective systems of first-order differential equations were resolved by the Eigenvalue method, minimizing χ^2. Statistical data are given as the mean ± S.E.M.

Results

Activation kinetics of CNGA2 channels depend on cGMP in a complex fashion

Activation of homotetrameric CNGA2 channels appeared in the time range of tens to hundreds of milliseconds (Fig. 3*A*). If cGMP binds to equivalent sites at the subunits *and* the binding limits the activation process, then

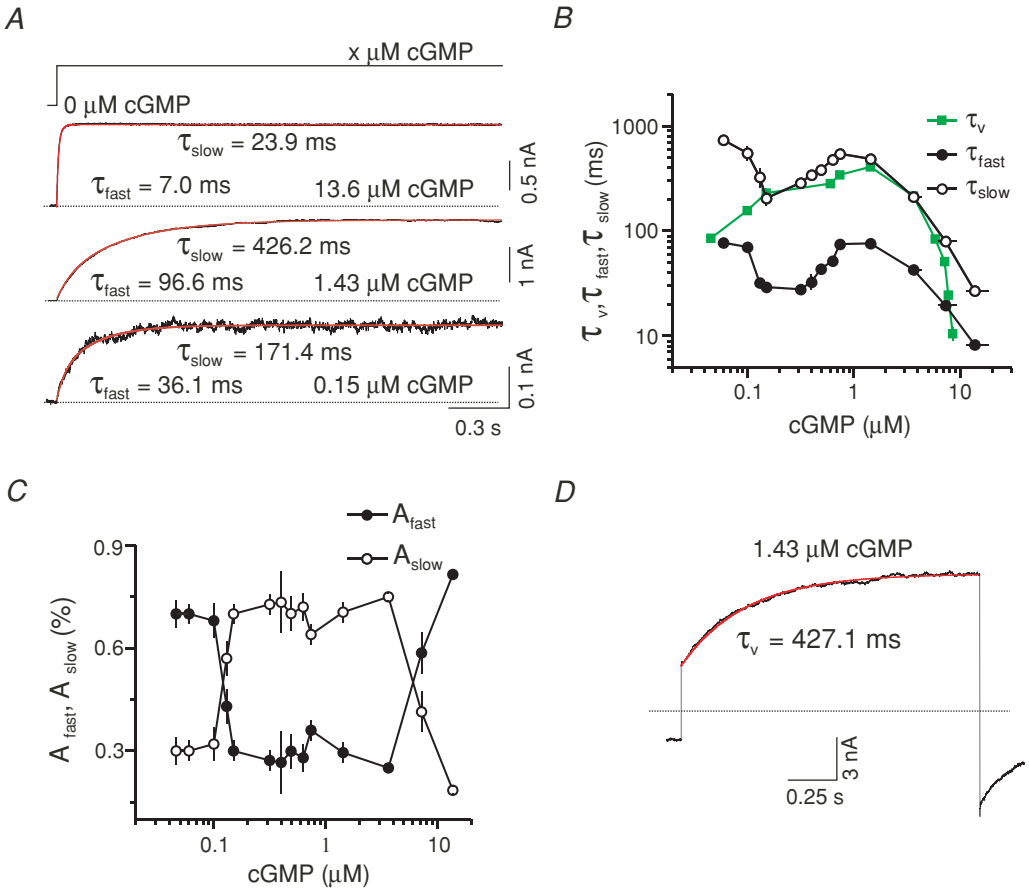

Figure 3. Activation of CNGA2 currents by cGMP and voltage
A, current traces at three cGMP jumps from zero to the indicated concentrations. The transmembrane voltage was +100 mV. The traces were fitted (red curves) with the sum of two exponentials yielding the indicated time constants τ_{fast} and τ_{slow}. At the intermediate concentration of 1.43 μM, the activation time course was slower than at higher and lower cGMP. *B*, plot of the activation time constants for cGMP jumps (τ_{fast}, τ_{slow}) and voltage steps (τ_v) as a function of the cGMP concentration. Each data point was obtained from 5 to 15 patches. Here, and in Figs 4*C* and 5*B*, the horizontal error bars indicate the 95% confidence interval for the cyclic nucleotide concentration as obtained from the fitted concentration–response curve at the respective concentration. *C*, relative contribution of the fast and slow exponential, A_{fast} and A_{slow}, to the activation time course for cGMP jumps. *D*, activation time course induced by a voltage step from −100 to +100 mV. The time course was fitted with a single exponential yielding the time constant τ_v.

the activation time course must be monotonically slowed in the direction to lower cGMP concentrations. However, activation at 0.15 μM cGMP was faster than at 1.43 μM cGMP (Fig. 3*A*). To investigate this result more thoroughly, the activation time course was studied over a wide range of cGMP concentrations and fitted with the sum of two exponentials, yielding the fast and slow time constants, τ_{fast} and τ_{slow}, and their relative contributions, A_{fast} and A_{slow}. Both time constants depend on the cGMP concentration as follows (Fig. 3*B*): they decrease when the concentration is raised from 0.06 μM to 0.15 μM, then increase until a concentration of 0.74 μM is reached, and decrease again to the highest concentrations.

The increase of the time constants at cGMP concentrations $> 0.15\,\mu$M shows that at all higher concentrations activation is not rate limited by the binding of cGMP to equivalent sites but by conformational changes of the channel. At the lowest cGMP concentrations ($< 0.15\,\mu$M), the decrease of the activation time constants with increasing cGMP suggests that other processes are rate limiting, which could be the diffusion of cGMP to the binding site and/or conformational changes at the binding site. Also the contribution of the fast and slow time constants depends on the cGMP concentration: the slow exponential dominates at intermediate cGMP concentrations whereas the fast exponential dominates at both high and low concentrations (Fig. 3*C*).

If the activation time course induced by cGMP jumps is rate limited by conformational changes of the channel, then any other stimulus that causes these conformational changes should generate a similar time course. At a constant cGMP concentration, structurally related CNGA1 channels were shown to be further activated on the millisecond time scale when the membrane voltage becomes depolarized (Benndorf *et al.* 1999). We compared for CNGA2 channels the activation time course induced by depolarization to that induced by cGMP jumps. Stepping from −100 to +100 mV generated currents with pronounced activation (Fig. 3*D*). In contrast to the results obtained with concentration jumps, the activating component could be described with a single time constant τ_v, which depends on the cGMP concentration in a bell-shaped fashion (Fig. 3*B*). At intermediate cGMP concentrations, τ_v approximates τ_{slow} whereas at both low and high cGMP τ_v is similar to τ_{fast}. Hence, τ_v is always similar to the dominating time constant of the cGMP-jump-induced activation (cf. Fig. 3*C*), suggesting that conformational changes of transmembrane channel parts are essentially involved in rate-limiting the activation time course over the whole range of cGMP concentrations, including the lowest. The fact that τ_v does not increase towards the lowest cGMP concentrations, as did τ_{fast} and τ_{slow} for cGMP jumps (Fig. 3*B*), suggests that at these low cGMP concentrations the rate-limiting processes are outside the transmembrane field and are also not closely coupled to voltage-dependent processes of transmembrane channel parts.

Activation kinetics of CNGA2 channels by cAMP and cGMP jumps are largely similar

The results so far do not allow us to decide whether at the low cGMP concentrations the binding of the cyclic nucleotide also contributes to the rate-limiting processes in activation. To address this point we performed experiments with cAMP, which produces a 26 times higher EC_{50} value than cGMP (Fig. 2*C*) but has an equal efficiency in opening the channels (Gordon & Zagotta, 1995) and should diffuse similarly fast. If the increase of τ_{fast} and τ_{slow} towards the lowest cGMP concentrations (Fig. 3*B*) is caused by conformational changes of the channel, then cAMP should shift the profile of τ_{fast} and τ_{slow} simply to higher concentrations by the factor $EC_{50,cAMP}/EC_{50,cGMP}$. Conversely, if the binding of the cyclic nucleotide is rate limiting, then cAMP should produce slower activation time courses than cGMP and this difference should be maximal at the lowest open probability (P_o).

Figure 4*A* shows that at low but similar values of P_o, jumps of cAMP and cGMP produce similar activation time courses. We determined the profiles for τ_{fast} and τ_{slow} over a wide cAMP range (Fig. 4*B*) and the result was that at the lowest measurable currents similar time constants were obtained at about 25 times higher concentrations compared to cGMP (Fig. 4*C*). When plotting τ_{fast} and τ_{slow} for both cyclic nucleotides as function of P_o (Fig. 4*D*), both relationships superimpose at low cyclic nucleotide concentrations. Hence, also at the lowest concentrations of the cyclic nucleotide, not the binding reactions but conformational changes of the channel are rate limiting for the activation process.

The diagrams also show that the whole profiles of τ_{fast} and τ_{slow} are approximately similar for both cyclic nucleotides, including the maximum near the EC_{50} value. In line with the above hypothesis, this result suggests that with both cyclic nucleotides the activation time course is rate limited by similar conformational changes of the channel and that the main difference between both cyclic nucleotides for the gating arises from different affinities. Besides the overall similarity of the activation time constants with cAMP and cGMP, they significantly differ at $0.03 < P_o < 0.4$ (Fig. 4*D*), suggesting that the cyclic nucleotides slightly modulate the conformational changes following the binding.

Activation kinetics of CNGA2/A4/B1b and CNGA2 channels by cAMP jumps are equally fast

We further tested whether the results so far reflect properties of native olfactory channels, which are heterotetramers with a subunit composition

CNGA2 : CNGA4 : CNGB1b of 2 : 1 : 1 (Zheng & Zagotta, 2004). The resulting EC_{50} value with free cAMP was 4.53 μM (Fig. 2*D*) which is similar to that for recombinant heterotetrameric (Sautter *et al.* 1998; Bönigk *et al.* 1999; Bradley *et al.* 2001) and native olfactory channels (Frings *et al.* 1992; Bönigk *et al.* 1999; Bradley *et al.* 2001). Activation time courses were elicited by cAMP jumps. As for CNGA2 channels, the time courses were slower near the EC_{50} value than at higher and lower cAMP concentrations (Fig. 5*A*). The profiles of τ_{fast} and τ_{slow} as a function of the cAMP concentration were similar to those obtained for CNGA2 channels (Fig. 5*B*). With respect to the EC_{50} value, both time constants are the same in heterotetrameric and homotetrameric channels when activated by cAMP (Fig. 5*C*). These results are intriguing because they suggest that in heterotetrameric and homotetrameric channels the main gating reactions are the same, though two of the four subunits differ (Zheng & Zagotta, 2004). Possible explanations are that the CNGA4 and CNGB1b subunit contribute similarly to the allosteric transition like their CNGA2 counterparts in homotetrameric channels. Alternatively, the CNGA4 and/or the CNGB1b subunit could not be involved in the allosteric transition. Because of the similarity of the activation time course in homo- and heterotetrameric channels, this would mean in turn that also in homotetrameric channels activation is rate limited by either two or three subunits only.

Modelling the activation time course of CNGA2 channels with kinetic schemes

To gain information upon the number of subunits contributing to the gating and the degree of cooperativity of the ligand binding, activation time courses

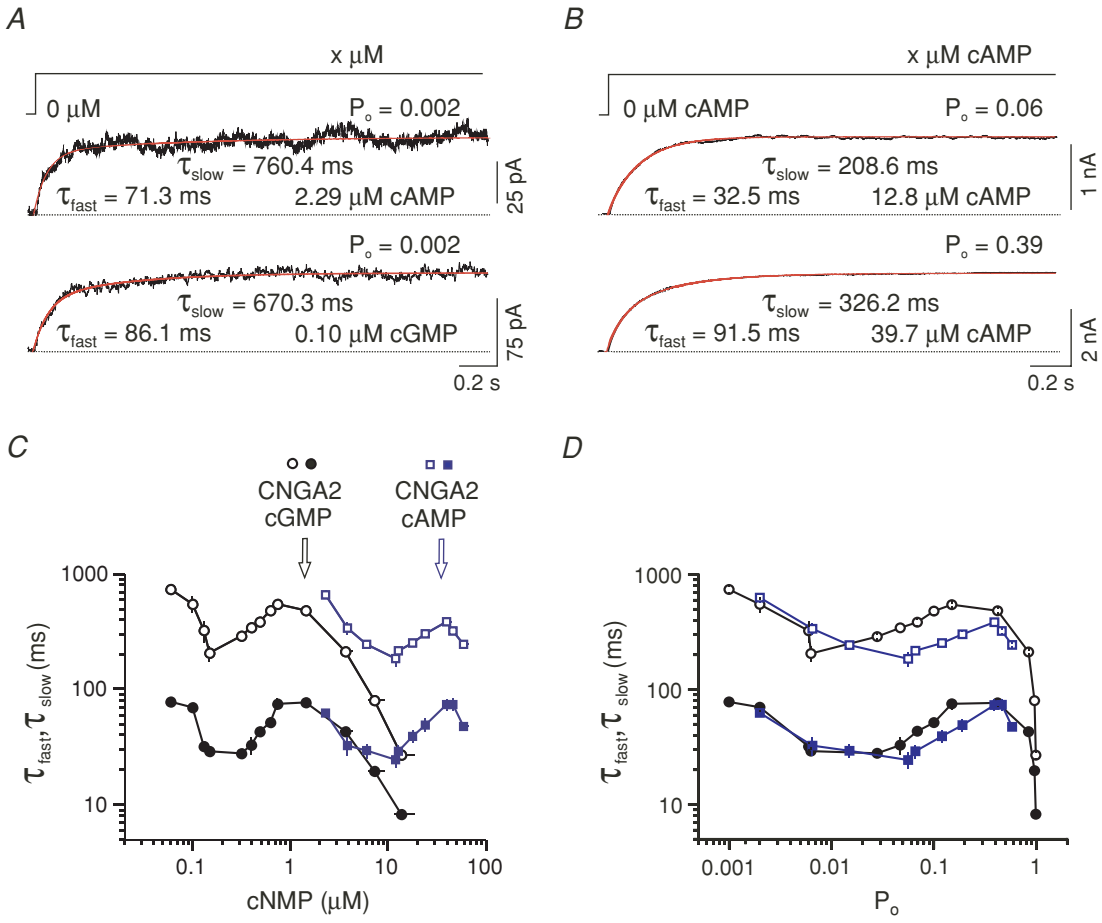

Figure 4. Activation of homotetrameric CNGA2 channels by cAMP jumps at +100 mV
The traces were fitted with the sum of two exponentials yielding τ_{fast} and τ_{slow}. *A*, current traces at low P_o are similarly fast with cAMP and cGMP. *B*, current traces at two cAMP concentrations. At the higher cAMP concentration of 39.7 μM, activation was slower than at the lower concentration of 12.8 μM. *C*, plot of τ_{fast} (filled symbols) and τ_{slow} (open symbols) as a function of the cAMP concentration. Each data point was obtained from 7–13 patches. The relationships are shifted to higher concentrations with respect to those obtained with cGMP. *D*, plot of τ_{fast} and τ_{slow} as function of P_o. The relationships are similar for cAMP and cGMP. Same symbols as in (*C*). The horizontal error bars have been omitted.

were analysed by fitting kinetic models. The analysis was performed for homotetrameric CNGA2 channels activated by jumps of cGMP because this combination provided data over the widest concentration range. The number of parameters in the fits was kept low by determining the open probability, P_o, and the mean open time, τ_o, at both zero and saturating cGMP (100 μM) directly (Fig. 6). Assuming that at both conditions each model is reduced to a two-state model according to

$$C \underset{k_{OC}}{\overset{k_{CO}}{\rightleftharpoons}} O \qquad \text{(Scheme 1)}$$

the rate constants k_{CO} and k_{OC} can be calculated (Table 1). The models were globally fitted to seven time courses of P_o following activation covering a wide range of cGMP concentrations.

Fit of a MWC model with the binding of four ligands to equivalent sites (Goulding *et al.* 1994) shows that this type of model is inconsistent because it predicts pronounced sigmoidal activation whereas the experimental data are biexponential (Fig. 7*A*). A similar negative result with too much sigmoidicity was obtained when fitting the coupled dimer (CD) model (Liu *et al.* 1998) (Fig. 7*B*). It should be emphasized, that both models could fully describe the steady-state currents alone (not shown).

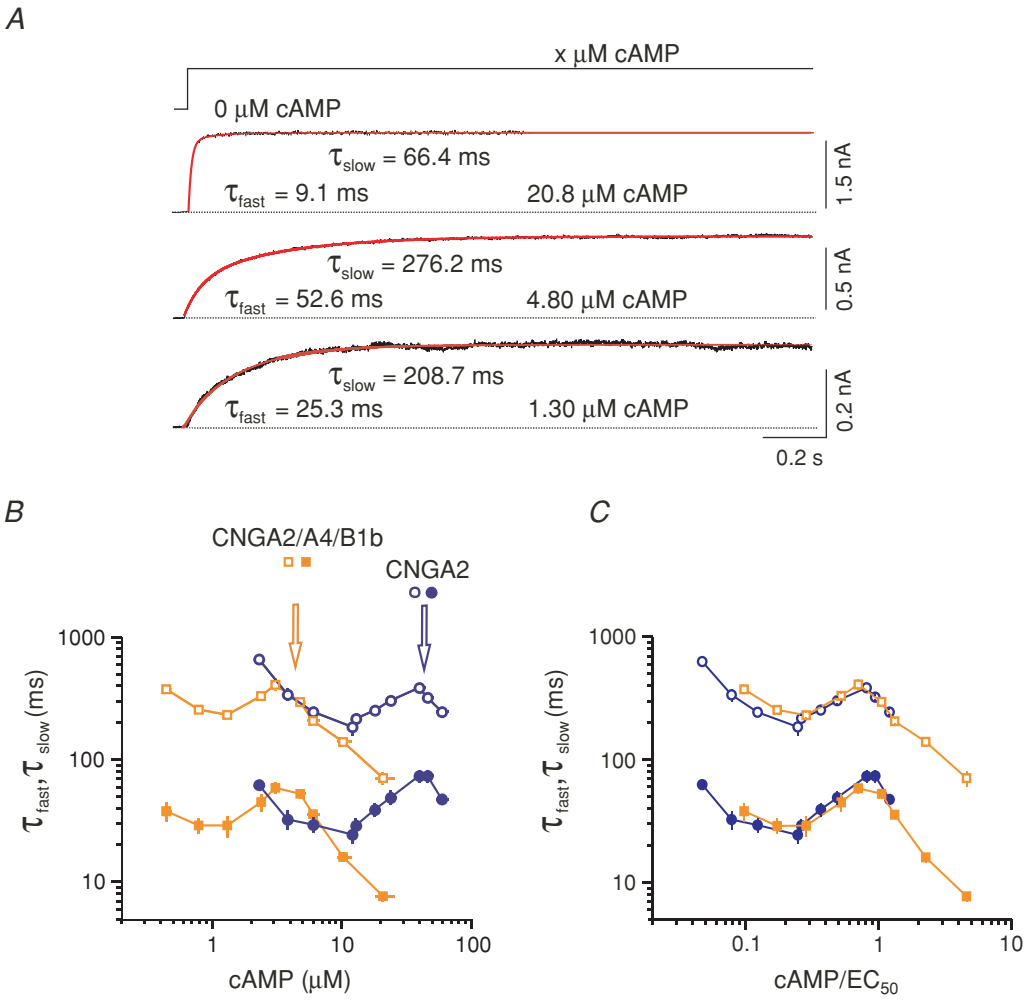

Figure 5. Activation of heterotetrameric CNGA2/A4/B1b channels by cAMP jumps at +100 mV
The traces were fitted with the sum of two exponentials yielding τ_{fast} and τ_{slow}. *A*, current traces at three cAMP concentrations. At the intermediate cAMP concentration of 4.80 μM, activation was slower than at the lower concentrations of 1.30 μM and the higher concentration of 20.8 μM. *B*, plot of τ_{fast} (filled symbols) and τ_{slow} (open symbols) as function of the cAMP concentration. Each data point was obtained from 6–15 patches. The relationships are shifted to lower cAMP concentrations with respect to those obtained with homotetrameric CNGA2 channels. *C*, plot of τ_{fast} and τ_{slow} as a function of the normalized EC_{50} value. The relationships for CNGA2 and CNGA2/A4/B1b channels superimpose completely. Same symbols as in *B*. The horizontal error bars have been omitted.

Table 1. Single-channel parameters at zero and saturating cGMP

	τ_o (ms)	P_o	k_{CO} (s^{-1})	k_{OC} (s^{-1})	No. of patches
No cyclic nucleotide	1.11 ± 0.08	$1.2 \times 10^{-4} \pm 1.4 \times 10^{-5}$	0.1	909	7
100 μM cGMP	93.2 ± 10.6	0.990 ± 0.001	1062	10.7	5

At 0 μM cGMP, two open times, τ_{o1} and τ_{o2}, were observed. For simplification of the analysis, the mean open time τ_o was calculated according to $\tau_o = (A_1\tau_{o1}^2 + A_2\tau_{o2}^2)/(A_1\tau_{o1} + A_2\tau_{o2})$. A_1 and A_2 are the respective amplitudes of the exponentials. At saturating cGMP (100 μM), only one open time component was observed yielding τ_o. P_o is the open probability. The rate constants were determined from the means according to $k_{CO} = P_o/[\tau_o(1 - P_o)]$ and $k_{OC} = 1/\tau_o$.

Similar inconsistency was obtained with 11 variants of the MWC and seven variants of the CD model, which all produced too much sigmoidicity.

We therefore considered cooperative models with unequal binding sites. Models with three binding steps were significantly superior over those with only two binding steps and models with four binding steps were 'reduced' by the fit to models with three binding steps. Among models with three binding steps, those with ligand binding only in the closed states were superior to those with ligand binding in both closed *and* open states. In total 78 models were tested. The cooperative three-state model with the best fit (Fig. 8*A* and *B*) includes pronounced negative and positive cooperativity: The first binding step is fast and does not lead to noticeable opening. The second binding step is by three orders of magnitude slower but switches to a state from which opening is extremely promoted. The third binding step is fast again and channel opening is similarly stabilized as for the double-liganded channel. Figure 8*C* shows the statistical result for the rate constants obtained from four sets of activation time courses. The conclusion is remarkably simple: the sequence of the ligand affinity for the three binding steps is high–low–high and only the second binding step switches the open probability from low to high values.

Discussion

Our experimental strategy allowed us to generate activation time courses with sufficiently high resolution to examine gating models assuming equivalent binding sites, among them the MWC (Monod *et al.* 1965; Goulding *et al.* 1994; Varnum & Zagotta, 1996) and the CD model

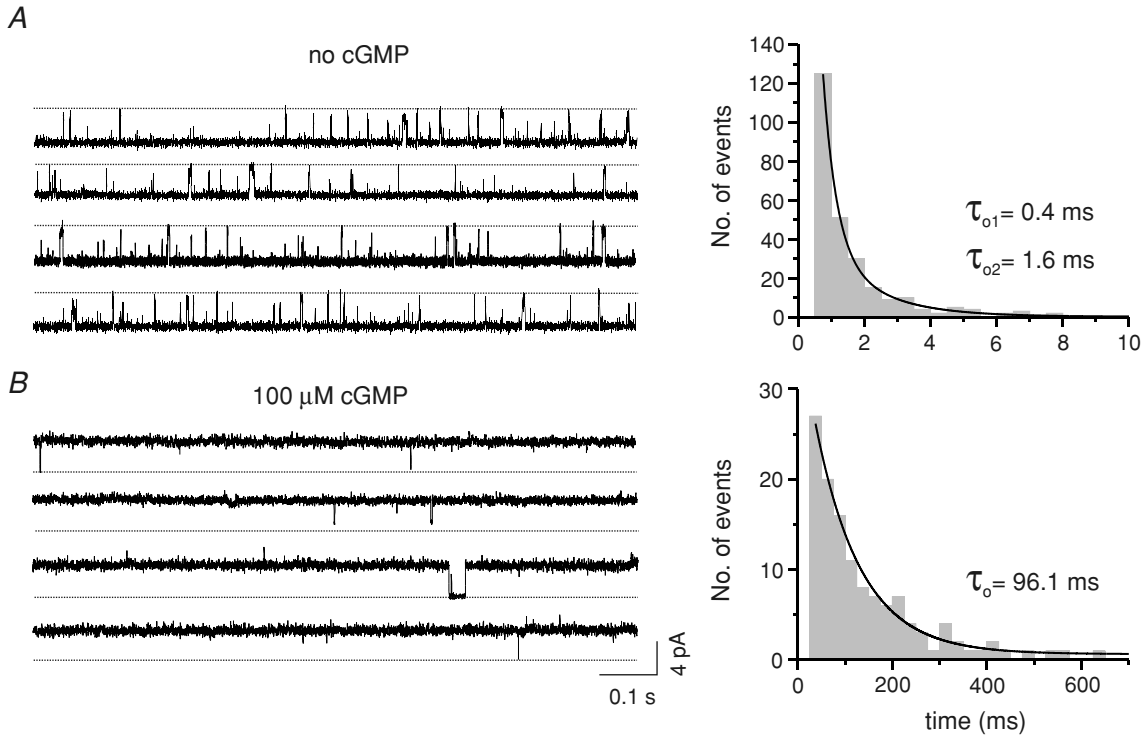

Figure 6. Gating kinetics of CNGA2 single channels at zero and saturating cGMP
A, 0 μM cGMP, multichannel patch (~175 channels). The open-time histogram yielded two time constants, τ_{o1} and τ_{o2}. *B*, 100 μM cGMP, single-channel patch. The open times distributed monoexponentially.

(Liu *et al.* 1998). The result was that these models are inadequate because they predict pronounced sigmoidicity of the activation time course which was not observed in the recordings (Fig. 7*B*). Hence, our strategy was substantially more stringent than previous strategies in which only steady-state currents were used to discriminate between gating models (Goulding *et al.* 1994; Varnum & Zagotta, 1996). Also with respect to single-channel analysis, our approach provides a key advantage because it is based on the mean activity of a great number of channels whereas single-channel activity varies in time (Li & Lester, 1999).

The inconsistency with the CD model is particularly intriguing because there is considerable evidence that proteins containing cyclic nucleotide binding domains form dimers. In the catabolite activator protein (CAP) of *Escherichia coli*, dimerization is caused through a coiled-coil interaction between the C-helices of the CNB domain (Weber & Steitz, 1997). In cyclic nucleotide regulated channels of the bacteria *Mesorhizobium loti* and *Rhodopseudomonas palustris*, an interaction of two N-terminal helices (αA and αA′) of two CNB domains has been shown to mediate dimerization and the same dimer interface has been identified in liganded and unliganded domain structures (Clayton *et al.* 2004). These authors postulate that the CNB domain dimers exist also in the channels and in both the open and closed states. Functional support for the formation of a dimer of dimers comes from single-channel data in CNGA1 channels with one, two, three, or four functional binding sites (Liu *et al.* 1998). These results are in contrast to structural data on isolated CNB domains of HCN2 channels, which belong to the class of hyperpolarization-activated cyclic nucleotide-gated (HCN) channels (Ludwig *et al.* 1998; Gauss *et al.* 1998). The CNB domains of HCN2 channels

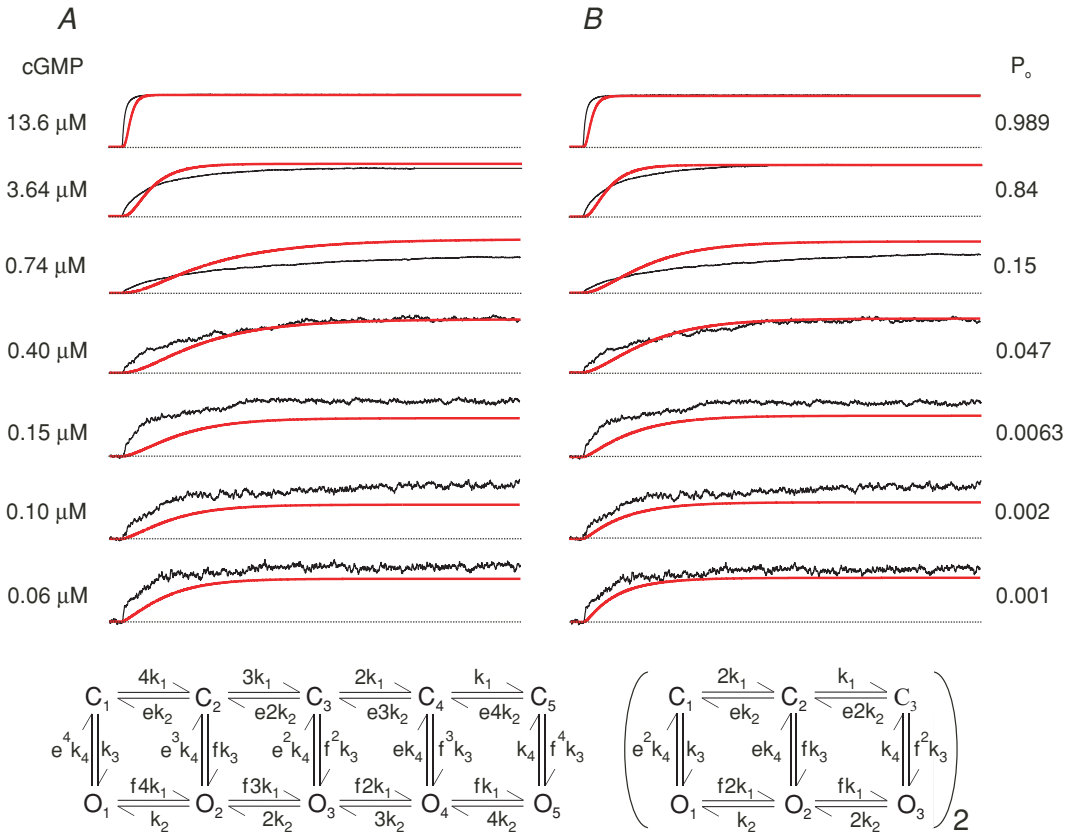

Figure 7. Kinetic models with independent ligand binding are inadequate to describe the time courses of cGMP-jump induced activation

The models were globally fitted to the indicated traces representing the time course of P_o following channel activation. 'O_x' and 'C_x' are open and closed states. *A*, Monod-Wyman-Changeux (MWC) model with four binding steps. From the open probability (P_o) and mean open time (τ_o) at zero (0) and saturating cGMP (sat), the rate constants k_3 and k_4 were determined from the relations $P_o(0) = k_3/(k_3 + e^4k_4)$, $\tau_o(0) = 1/e^4k_4$, $P_o(\text{sat}) = f^4k_3/(f^4k_3 + k_4)$, $\tau_o(\text{sat}) = 1/k_4$. To solve these equations, two different allosteric parameters, e and f, had to be attributed to the opening and closing transition. Using the values from Table 1, the results were $k_3 = 1.09 \times 10^{-1}\ \text{s}^{-1}$, $k_4 = 10.73\ \text{s}^{-1}$, $f = 9.94$, $e = 3.03$. The best fit yielded $k_1 = 3.03\ \mu\text{M}^{-1}\ \text{s}^{-1}$ and $k_2 = 3.24\ \text{s}^{-1}$. *B*, coupled-dimer (CD) model. Each dimer can bind two ligands and the channel is assumed to be open only if both dimers are in an open state. The rate constants k_3 and k_4 were determined from the relations $P_o(0) = [k_3/(k_3 + e^2k_4)]^2$, $\tau_o(0) = 1/2e^2k_4$, $P_o(\text{sat}) = [f^2k_3/(f^2k_3 + k_4)]^2$, $\tau_o(\text{sat}) = 1/2k_4$. The results were $k_3 = 5.03\ \text{s}^{-1}$, $k_4 = 5.36\ \text{s}^{-1}$, $f = 14.52$, $e = 9.19$. The best fit yielded $k_1 = 2.8\ \mu\text{M}^{-1}\ \text{s}^{-1}$ and $k_2 = 4.6\ \text{s}^{-1}$.

form a ring-like tetrameric structure when cAMP is present and do not interact appreciably as compared to the subunits in CAP (Zagotta *et al.* 2003) and the bacterial channels (Clayton *et al.* 2004) though the respective structural elements are present. Only in the absence of cAMP is there evidence that dimers are also formed. It is therefore not finally answered to what extent dimerization is functionally relevant. It should be noted that the data of the present study do not necessarily conflict with a structure of a dimer of dimers when only the binding is sufficiently cooperative.

A symmetric tetrameric structure of homotetrameric CNGA2 channels is very likely not only from the crystals of the binding domains of bacterial cyclic nucleotide regulated channels (Clayton *et al.* 2004) and HCN channels (Zagotta *et al.* 2003), but also from the complete structures of K^+ channels (Doyle *et al.* 1998; Jiang *et al.* 2003*a*,*b*) which are also related to CNG channels (Yellen, 2002). How then is it possible that in a symmetric homotetrameric channel three of the four subunits are selected for the gating? A simple explanation is that the binding of the first ligand itself generates the asymmetry by decelerating the binding step in the other subunits in a sense of negative cooperativity. Once the second ligand binds, the affinity for the third ligand would be strongly increased while the binding site of the fourth subunit is without great effect. Taking into account that native CNG channels contain one B subunit, the assumption of only three gating subunits is not so surprising because one may speculate that evolution specialized the fourth subunit to a B subunit to modulate the channel function, as e.g. shown for the CNGB1b subunit by calmodulin complexed with Ca^{2+} ions (Bradley *et al.* 2001, 2004). For native olfactory channels, this consideration assumes that the CNGA4 subunit also contributes to the gating.

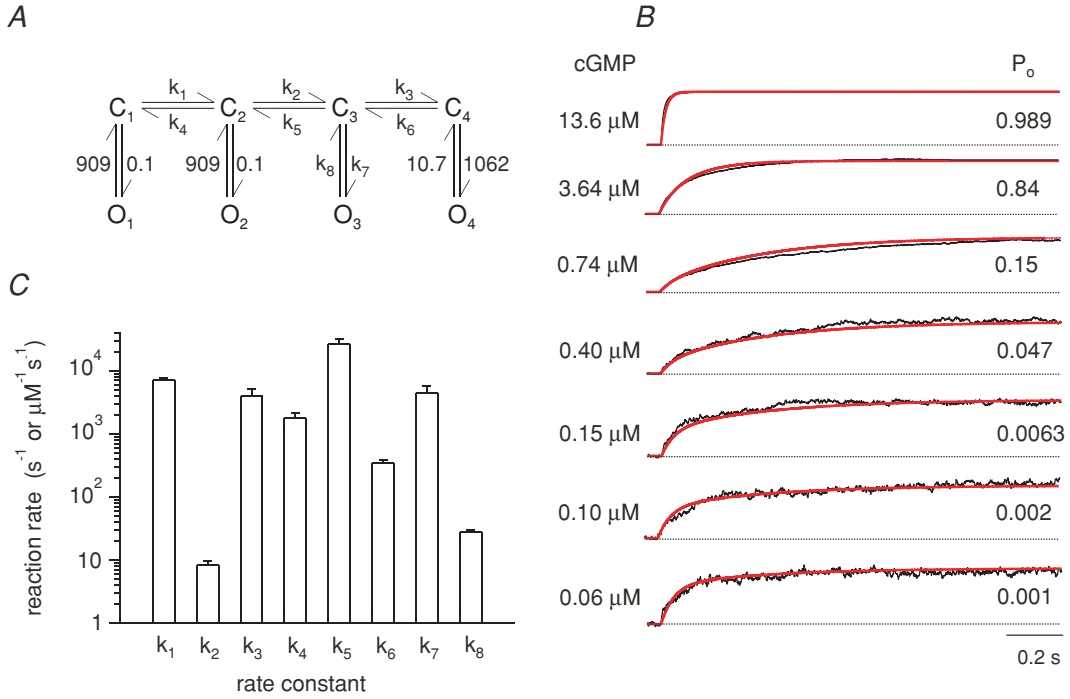

Figure 8. Fit of CNGA2 activation time courses induced by cGMP jumps with the cooperative three-state model

A, scheme. 'O_x' and 'C_x' are open and closed states. The numbers indicate rate constants with the units $\mu M^{-1}\ s^{-1}$ for the binding steps and s^{-1} for all other transitions. *B*, seven time courses of P_o covering a wide range of concentrations were globally fitted (red curves) yielding the rate constants indicated in the scheme (*A*). The open times and P_o for the non-liganded and the fully liganded channel were determined from single-channel recordings (Table 1 and Fig. 6). The rate constants for the transition $C_2 \rightleftharpoons O_2$ were equated to those of the transition $C_1 \rightleftharpoons O_1$ because fitting reduced the open probability of the single liganded channel consistently to lower values than that of the nonliganded channel. The results were $k_1 = 6.0 \times 10^3\ \mu M^{-1}\ s^{-1}$, $k_2 = 6.5\ \mu M^{-1}\ s^{-1}$, $k_3 = 2.6 \times 10^3\ \mu M^{-1}\ s^{-1}$, $k_4 = 1.4 \times 10^3\ s^{-1}$, $k_5 = 1.4 \times 10^4\ s^{-1}$, $k_6 = 3.5 \times 10^2$, $k_7 = 2.8 \times 10^3\ s^{-1}$, $k_8 = 2.6 \times 10^1\ s^{-1}$. The model describes both the activation time courses and the steady-state currents (concentration–response relationship) adequately. *C*, mean of reaction rate constants calculated from four sets of activation time courses. k_1 to k_3 are given in $\mu M^{-1}\ s^{-1}$, k_4 to k_8 in s^{-1}. Error bars indicate S.E.M.

References

Benndorf K, Koopmann R, Eismann E & Kaupp UB (1999). Gating by cyclic GMP and voltage in the α subunit of the cyclic GMP-gated channel from rod photoreceptors. *J General Physiol* **114**, 477–489.

Bönigk W, Bradley J, Muller F, Sesti F, Boekhoff I, Ronnett GV *et al.* (1999). The native rat olfactory cyclic nucleotide-gated channel is composed of three distinct subunits. *J Neurosci* **19**, 5332–5347.

Bradley J, Bönigk W, Yao K-W & Frings S (2004). Calmodulin permanently associates with rat olfactory CNG channels under native conditions. *Nature Neurosci* **7**, 705–710.

Bradley J, Reuter D & Frings S (2001). Facilitation of calmodulin-mediated odor adaptation by cAMP-gated channel subunits. *Science* **294**, 2176–2178.

Clayton GM, Silverman R, Heginbotham L & Morais-Cabral JH (2004). Structural basis of ligand activation in a cyclic nucleotide regulated potassium channel. *Cell* **119**, 615–627.

Doyle DA, Morais-Cabral JH, Pfuetzner RA, Kuo A, Gulbis JM, Cohen SL *et al.* (1998). The structure of the potassium channel: Molecular basis of K^+ conduction and selectivity. *Science* **280**, 69–77.

Frings S, Lynch JW & Lindemann B (1992). Properties of cyclic nucleotide-gated channels mediating olfactory transduction. *J General Physiol* **100**, 45–67.

Gauss R, Seifert R & Kaupp UB (1998). Molecular identification of a hyperpolarization-activated channel in sea urchin sperm. *Nature* **393**, 583–587.

Gordon SE & Zagotta WN (1995). Localization of regions affecting an allosteric transition in cyclic nucleotide-activated channels. *Neuron* **14**, 857–864.

Goulding EH, Tibbs GR & Siegelbaum SA (1994). Molecular mechanism of cyclic-nucleotide-gated channel activation. *Nature* **372**, 369–374.

Hagen V, Bendig J, Frings S, Eckardt T, Helm S, Reuter D *et al.* (2001). Highly efficient and ultrafast phototriggers for cAMP and cGMP by using long-wavelength UV/Vis-activation. *Angew Chem* **40**, 1046–1048.

Jiang Y, Lee A, Chen J, Ruta V, Cadene M, Chait BT *et al.* (2003*a*). X-ray structure of a voltage-dependent K^+ channel. *Nature* **423**, 33–41.

Jiang Y, Ruta V, Chen J, Lee A & MacKinnon R (2003*b*). The principle of gating charge movement in a voltage-dependent K^+ channel. *Nature* **423**, 42–48.

Karpen JW, Zimmerman AL, Stryer L & Baylor DA (1988). Gating kinetics of the cyclic-GMP-activated channel of retinal rods: Flash photolysis and voltage jump studies. *Proc Natl Acad Sci U S A* **85**, 1287–1291.

Kaupp UB & Seifert R (2002). Cyclic nucleotide-gated ion channels. *Physiol Rev* **82**, 769–824.

Li J & Lester HA (1999). Single-channel kinetics of the rat olfactory cyclic nucleotide-gated channel expressed in *Xenopus* oocytes. *Molec Pharmacol* **55**, 883–893.

Li J, Zagotta WN & Lester HA (1997). Cyclic-nucleotide gated channels: structural basis of ligand efficacy and allosteric modulation. *Quart Rev Biophys* **30**, 177–193.

Liu DT, Tibbs GR, Paoletti P & Siegelbaum SA (1998). Constraining ligand binding site stoichiometry suggests that a cyclic nucleotide-gated channel is composed of two functional dimers. *Neuron* **21**, 235–248.

Ludwig A, Zong X, Jeglitisch M, Hofmann F & Biel M (1998). A family of hyperpolarization-activated mammalian cation channels. *Nature* **393**, 587–591.

Middendorf TR & Aldrich RW (2000). Effects of ultraviolet modification on the gating energetics of cyclic nucleotide-gated channels. *J General Physiol* **116**, 253–282.

Middendorf TR, Aldrich RW & Baylor DA (2000). Modification of cyclic nucleotide-gated ion channels by ultraviolet light. *J General Physiol* **116**, 227–252.

Monod J, Wyman J & Changeux JP (1965). On the nature of allosteric transitions: a plausible model. *J Mol Biol* **12**, 88–118.

Picones A & Korenbrot JI (1995). Spontaneous ligand-independent activity of the cGMP-gated ion channels in cone photoreceptors in fish. *J Physiol* **485**, 699–714.

Ruiz ML & Karpen JW (1997). Single cyclic nucleotide-gated channels locked in different ligand-bound states. *Nature* **389**, 389–392.

Sautter A, Zong X, Hofmann F & Biel M (1998). An isoform of the rod photoreceptor cyclic nucleotide-gated channel β subunit expressed in olfactory neurons. *Proc Natl Acad Sci U S A* **95**, 4696–4701.

Tibbs GR, Goulding EH & Siegelbaum SA (1997). Allosteric activation and tuning of ligand efficacy in cyclic-nucleotide-gated channels. *Nature* **386**, 612–615.

Varnum MD & Zagotta WN (1996). Subunit interactions in the activation of cyclic nucleotide-gated ion channels. *Biophys J* **70**, 2667–2679.

Weber IT & Steitz TA (1997). Structure of a complex of catabolite gene activator protein and cyclic AMP refined at 2.5 A resolution. *J Mol Biol* **198**, 311–326.

Yellen G (2002). The voltage-gated potassium channels and their relatives. *Nature* **419**, 35–42.

Zagotta WN, Olivier NB, Black KD, Young EC, Olson R & Gouaux E (2003). Structural basis for modulation and agonist specificity of HCN pacemaker channels. *Nature* **425**, 200–205.

Zagotta WN & Siegelbaum SA (1996). Structure and function of cyclic nucleotide-gated channels. *Ann Rev Neurosci* **19**, 235–263.

Zheng J & Zagotta WN (2004). Stoichiometry and assembly of olfactory cyclic nucleotide-gated channels. *Neuron* **42**, 411–421.

Acknowledgements

We are indebted to U. B. Kaupp for providing the clones and to T. Baukrowitz for comments on the manuscript. We would also like to thank A. Hertel, G. Sammler, K. Schoknecht, S. Bernhardt, A. Kolchmeier and B. Tietsch for excellent technical assistance. The work was also supported by the grant Be 1250/14-3 and the Graduiertenkolleg 'Biomolecular Switches' of the Deutsche Forschungsgemeinschaft.